Hanke, S.; Fischer, A.; dos Santos, J.F.:

Sliding wear behaviour of a Cr-base alloy after microstructure alterations induced by friction surfacing

In: Wear (2015) Elsevier

DOI: 10.1016/j.wear.2015.07.010

Sliding Wear Behaviour of a Cr-base Alloy after Microstructure Alterations Induced by Friction Surfacing

S. Hanke*[1], A. Fischer[2], J. F. dos Santos[1]
[1]*Helmholtz Zentrum Geesthacht, Institute of Materials Research, Materials Mechanics, WMP, Max-Planck-Straße 1, Geesthacht, Germany*
[2]*University of Duisburg-Essen, Materials Science and Engineering, Lotharstr.1, Duisburg, Germany*

Abstract

Friction surfacing is a method suitable to generate a wide variety of metallic coatings by means of frictional heating and severe shear deformation. It is a solid-state joining method, and therefore may be applied to non-fusion weldable as well as non-deformable brittle materials, as Cr-based alloys are. In the present study coatings of Cr60Ni40 alloy are generated onto Nimonic 80A substrates. Microstructural investigations of the coating material are carried out and compared to the usual cast state. The wear behaviour of the coatings as well as the cast material is examined under reciprocating sliding against 52100 ball bearing steel by means of a ball-on-flat test rig, lubricated with silicone oil to prevent oxidation. In this tribological system, wear takes place by abrasion with microploughing being the predominant submechanism, surface fatigue as well as adhesion by materials transfer of Cr60Ni40 from the flats to the steel balls. White etching layers form on Cr60Ni40 underneath the worn surfaces, which show cracks and delaminations. The amount of wear of all coatings is within the same magnitude compared to the cast state but slightly smaller. This can be explained by the distinctly finer microstructure (grain boundary strengthening) and a high degree of supersaturation of the solid solutions (solid solution strengthening) within the coatings. The results of this study show that it is possible to generate coatings of brittle alloys like Cr60Ni40 by friction surfacing, which show a slightly better wear behaviour under reciprocating sliding. Thus, in combination with a ductile substrate, these coatings are likely to extend the range of applicability of such high-temperature wear and corrosion resistant alloys.

Keywords: solid-state joining, hardfacing, thermomechanical processing, non-ferrous metals, sliding wear

1. Introduction

Friction surfacing is a solid-state joining method, in which the required heat is generated by friction and the bonding is achieved under the applied forging pressure. A rotating rod made from the coating material is pressed with a defined axial force onto the substrate, and the friction in the contact causes heating of both rod and substrate material. When the heat flow into the system and the surroundings is adequate, the temperature maximum is located within the rod tip, and the acting frictional torque causes the thermally softened material to flow. Now, the relative

*Corresponding author. Tel.: +49 4152 87 2032; fax: +49 4152 87 2033.
E-mail address: stefanie.hanke@hzg.de (Stefanie Hanke)

motion between the rotating rod and substrate shifts from the sliding interface to the shear plane of the thermally softened rod material [1]-[4]. When this state is reached after a certain period of time (pre-heating phase), a translational movement is superimposed, either by guiding the rotating rod over the substrate, or by shifting the substrate's position. Along the trajectory, part of the softened material from the rod tip is transferred onto the substrate and a coating of a width similar to the rod diameter remains. Another part of the soft material, from the periphery of the rod, is squeezed out of the contact zone by the axial force, and is pushed upwards around the rod forming a flash. Also, since the soft material at the outer edge of the rod cannot carry the axial forging force, a lack of fusion is present in a narrow region along the edges of each coating layer, which is characteristic for friction surfacing. The length of a single coating layer is limited by the availability of coating material from the rod, as for any other welding consumable, but its efficiency is further decreased by the flash [3] [5] [6]. Thickness and width of the coating layer, as well as the bonding quality, are affected by the process parameters, most importantly by the axial force, the rotational and the translational speed. Additional factors like the surrounding temperature and atmosphere, cooling or heating measures also influence the outcome of the process [6] [7]. Coating layers can be applied on top of each other or in an overlapping manner, in order to obtain higher thicknesses or widths [1] [2] [8].

The process of friction surfacing can be applied to a wide variety of materials, and often results in a fine and homogenised microstructure within the coating. The reasons are the severe plastic shear deformation at forging temperature followed by immediate rapid cooling [5] [9]-[12].

Cr-Ni alloys with high Cr content are brittle and therefore regarded to be non-deformable and non-weldable and are available only as cast parts. Still, with increasing Cr content, the hardness and more important the high-temperature corrosion resistance improve significantly. In parallel the creep rupture strength as well as the ductility decrease [13]. Extensive studies concerning refinery furnaces in the 1960s showed that the severity of corrosion at temperatures up to 900°C is comparable for components from Cr50Ni50 and Cr60Ni40 alloys. For higher temperatures just the Cr60Ni40 alloy as defined by ASTM A560 (Table 1) showed a significant corrosion resistance [13] [14]. Thus, such alloys are applied for components suffering high-temperature corrosive impact, especially under simultaneous high-temperature wear.

C	Mn	Si	S	P	N	Fe	Ti	Al	Cr	Ni
< 0.1	< 0.1	< 1.0	< 0.2	< 0.2	< 0.3	< 1.0	< 0.5	< 0.25	58.0 – 60.0	balance
tensile strength > 760 MPa								yield strength > 590 MPa		

Tab. 1. Chemical composition and properties of Cr60Ni40 according to ASTM 560/A 560 M [14]

For the binary Chromium-Nickel system, usually three equilibrium solid state phases are denoted, being either an fcc Ni- or a bcc Cr-rich solid solution besides an ordered Ni_2Cr intermetallic phase present below 590°C [15] [16]. A eutectic exists, which reportedly ranges between 46 to 49 wt-% Ni and 1327 to 1345°C [13] [16] [17]. One feature important for the formation of phases in Cr-rich Cr-Ni-alloys is the low solubility of Ni in bcc-Cr at room temperature. While at the eutectic temperature approximately 35 wt-% Ni can be dissolved, this drops markedly with temperature leading to only 5 wt-% below 900°C followed by a further decrease to room temperature. Precise values for the solubility of Ni in Cr at room temperature are not given [15] [16]. It should be mentioned here that

besides the application as castings Cr-Ni alloys can also be found as thin sputtered films in microelectronics. These have been extensively studied leading to the identification of further non-equilibrium phases [15]-[21].

In the present study, coatings from Cr60Ni40 are generated onto a Nimonic 80A substrate by friction surfacing. The aim is to combine the high-temperature wear and corrosion resistance of the Cr-rich cast alloy with the much better combination of ductility and high-temperature strength of Ni-base superalloy substrates. The feasibility of friction surfacing in this material configuration has first been shown in [22], where the coatings' resistance to cavitation was investigated. In the current study, the wear behaviour of the coatings was examined by means of reciprocating sliding wear tests and compared to the as-cast state. The results are discussed in relation to the different microstructures.

2. Experimental Methods

2.1 Coating Process

For the coating process, sheets from Nimonic 80A alloy (ASTM B 637; 2.4631) were used as substrate material. This high-temperature alloy contains about 70 wt-% of Ni, 20 wt-% Cr and some small additions of Ti, Al and Fe. The surface of the sheets was ground for planarity and cleaned by degreasing with acetone.

Coatings were prepared out of rods from Cr60Ni40. At the beginning of the process, the rotating rod was pressed onto the substrate and kept without translational movement for 110 s. In this preheating period, the substrate was warmed up by the frictional heat and the material in the rod tip was sufficiently plasticized. The latter was assessed by measuring the shortening of the rod under the applied pressure being 3 mm during preheating. Parameters for the coating process are given in Tab. 2. Wider coatings were produced by overlapping several layers, without any additional surface preparation measures. A sample with three layers is presented in Fig. 1 (a).

rotational speed	3500 min^{-1}	rod diameter	20 mm
translational speed	0.33 m/min	thickness of substrate sheets	10 mm
axial force	28 kN	offset for overlapping layers	10 mm

Tab. 2. Friction surfacing parameters

2.2 Metallography and Microscopy

The rods used to produce the coatings by friction surfacing were machined from commercially available cast and heat treated components. Cross sections were prepared by standard metallographic methods from such material and examined by optical- (OM, BX41TF, Olympus Optical Co. Ltd., Tokyo, Japan) and scanning-electron-microscopy (SEM, Leo 1530 Gemini, Carl Zeiss Microscopy GmbH, Jena, Germany) including energy dispersive X-ray analysis (EDS, Apollo X10, EDAX Inc., Mahwah, NJ, USA). To reveal the microstructure the polished samples were etched

with a solution containing 100 ml HCl, 100 ml H_2O, 10 ml HNO_3 and 1 ml Dr. Vogels' etchant (Buehler GmbH, Düsseldorf, Germany), which contains propanol and thiourea. Cross sections of the single and overlapping coatings were prepared with the visible plane perpendicular to the welding direction, and in case of worn samples parallel to the sliding direction, by means of the same procedures. In order to investigate the material directly under the worn surfaces the samples were protected by an electroless Ni-plating (EdgeMet Electroless Nickel Kit, Buehler GmbH, Düsseldorf, Germany) before metallographic preparation of the cross sections.

2.3 Wear Tests

For reciprocating sliding wear tests samples with three overlapping layers were cut to a size of 30 x 20 mm and the surface of the coatings was ground until a plane of sufficient size was generated. These surfaces were then polished using diamond suspension down to a grain size of 1 µm (Fig. 1). Samples from cast Cr60Ni40 were taken from the identical cast rods and prepared accordingly. Surface preparation was carried out carefully using standard metallographic methods, in order not to affect the subsurface microstructure.

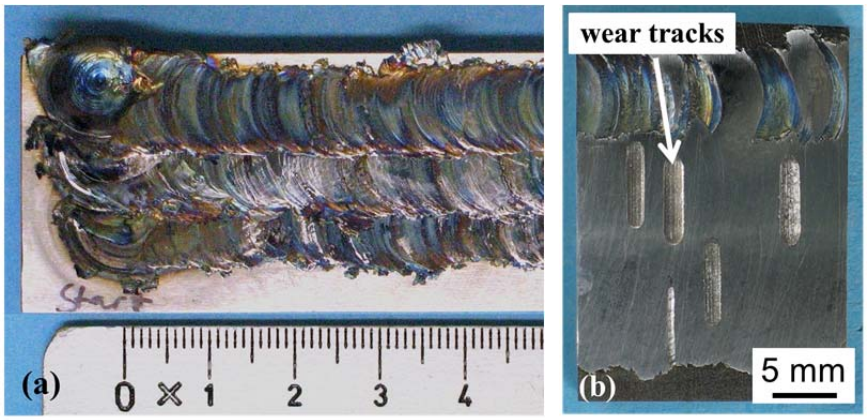

Fig. 1. Triple-layer coating (a) and FS coating sample after wear tests (b)

A ball-on-flat setup was used, in which the flat, which is made from the coated or cast samples, was positioned vertically and fixed to the traverse of the machine via a load cell. The ball was rubbed against the flat in reciprocating sliding also in vertical direction. Cr60Ni40 components are faced with steel or Ni-superalloy counterbodies in applications involving tribological loading. In the present investigation, standard bearing balls (100Cr6; 1.3505; AISI 52100) of 10 mm diameter were chosen as counterbodies, because they are available in high quality (homogeneity of microstructure, hardness, surface finish and accuracy of shape) from roller bearing producers. All tests were run at room temperature under uncontrolled ambient conditions and lubricated with silicone oil (M50, Carl Roth GmbH, Karlsruhe, Germany) to avoid oxidation in the contact. The oil has a viscosity of 45-55 mm^2/s and a density of 0.96-0.97 kg/m^3 according to the manufacturer's data sheet. The lubricant was fed into the contact by continuous dripping.

The sliding motion of the balls was generated by a servo hydraulic test-rig, while the normal force is applied by means of metal springs. The test parameters included a frequency of 6 Hz at an amplitude of 3 mm, resulting in an average relative velocity of 4.3 m/min. The tests were run for 12,500 and 25,000 cycles, corresponding to 75 m and 150 m total sliding distance, under normal loads of 45 and 60 N. This corresponds to a Hertzian pressure at the start of the test runs of 1,110 MPa and 1,220 MPa. Each set of parameters was tested two or three times and the average as well as the standard deviation of measured data were calculated.

During the experiments, normal and tangential (friction) forces were measured in order to gain the coefficient of friction and to monitor the steadiness of the wear behaviour. After the tests were finished, the samples were cleaned in acetone. Following cleaning, the wear volume of each sample was determined using confocal microscopy (µSurf, NanoFocus AG, Oberhausen, Germany). Additionally, scanning-electron-microscopy was used to identify the wear mechanisms of both the flats and the balls.

3. Results

3.1 Microstructure

The macroscopic hardness measured 5 times on each sample by the Vickers' method is 480 ± 21 HV5 for the coatings and 430 ± 8 HV5 for the cast material. The microstructure evolution during friction surfacing of Cr60Ni40 has already been discussed in [22] and shall only be summed up here.

The cast material shows a characteristic dendritic microstructure with Cr-rich (≈ 59 wt-% Cr determined by EDS) darker areas which also show an uneven colouring due to the presence of fine, lamellar precipitates. Due to the rapid decrease of the solubility of Ni in Cr with temperature, the regions of primary Cr-rich solid solution (dark) contain a Ni-rich phase (bright areas) from segregation during cooling. The much larger brighter regions in between the Cr-rich dendrites also show fine lamellae, but now from eutectic solidification (47 to 50 wt-% Cr) (Fig. 2 (a)).

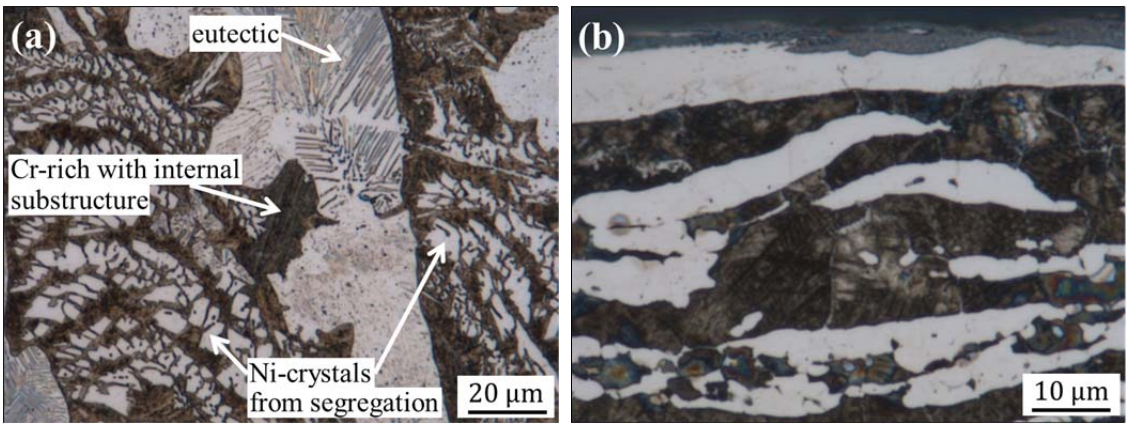

Fig. 2. Microstructure of Cr60Ni40 in cast state (a) and after friction surfacing, adjacent to the coating's surface (b)

The microstructure of Cr60Ni40 after processing by friction surfacing is presented in Fig. 2 (b) at a twofold higher magnification. It is obvious, that the microstructure of the coating is significantly finer than that of the cast state. Now, no precipitates or eutectic lamellae are present within the brighter areas (≈ 52 wt-% Cr by EDS), while the darker, Cr-rich (≈ 63 wt-% Cr) regions contain less Ni-rich crystals compared to the cast material. An irregular greyish oxide layer of up to 20 µm thickness is visible on the surface of the coating (Fig. 2 (b)). Such oxide layers were removed before wear testing during sample preparation by grinding and polishing, and therefore do not affect the wear behaviour.

3.2 Wear Behaviour

The average friction coefficients calculated from the measured normal and tangential forces are 0.32 ± 0.01 (60 N) and 0.29 ± 0.02 (45 N) independent of the type of material in the test.

Wear scars on the flats are trough shaped, as shown in the 3D image in Fig. 3. Grooves parallel to the sliding direction and a small amount of material build-up around the wear scar are visible. The volume of the trough (wear volume) can be determined from the measured topographical data, and the values for the different test parameters are presented in Fig. 4 (a). The wear volume of the Cr60Ni40 material increases both with the normal force and the number of cycles for the cast material and the coatings, while the coatings always show a slightly lower value. In Fig. 4 (b), the wear rates averaged over the complete test duration are given, calculated by dividing the measured values from Fig. 4 (a) by the corresponding normal force and total sliding distance. These values therefore include a potential run-in and any other change in wear behaviour throughout the test. Although there is an overlap of the error bars, there is a tendency of the wear rate to increase with test duration for 45 N normal force, and it further rises for 12,500 cycles at 60 N normal force. For the longer test duration at the high normal force, the wear rate is lower. Again this trend is true for both material states, with the FS coatings always displaying a lower value, than the as-cast state.

For the steel balls, the wear volume was too small to be determined by this method.

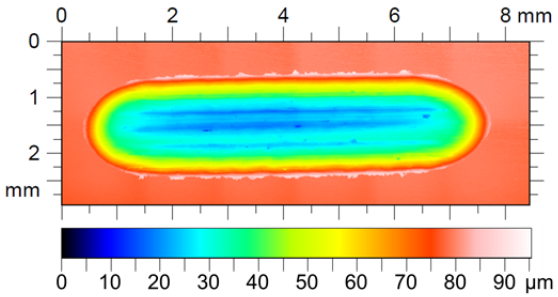

Fig. 3. Wear scar on cast Cr60Ni40 measured by confocal light microscopy: 60N; 12,500 cycles

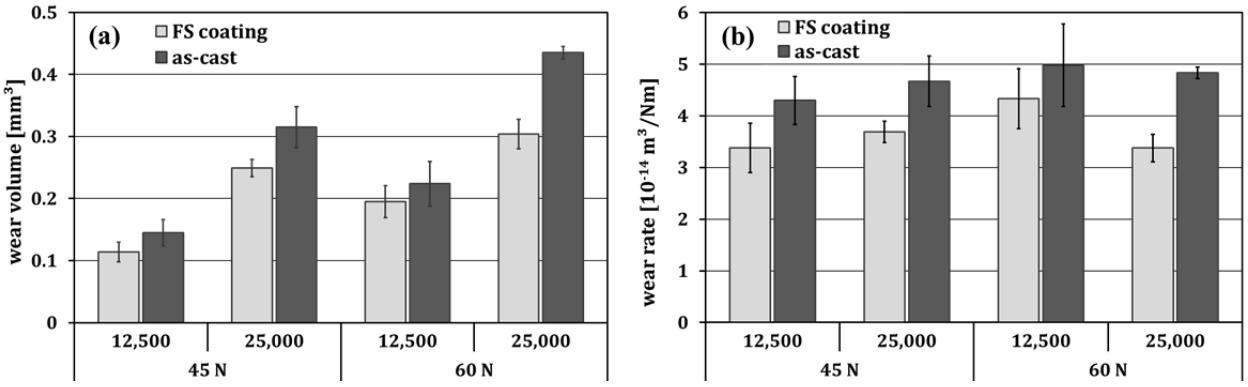

Fig. 4. Wear volumes (a) and average wear rates (b) of the flats over normal force and number of cycles

In Fig. 5 and Fig. 6 SEM images of a pair (flat and ball) of worn surfaces from a wear test under 60 N for 25,000 cycles are presented. The trough shaped wear scar on the flat shows grooves and some delaminations (Fig. 5). Compact inclusions are also visible, which have not been damaged during the wear test (Fig. 5 (b)). On the ball, within the elliptical wear scar, also some grooves are visible. At a higher magnification it becomes obvious, that small beads of material adhere to the otherwise rather smooth ball surface (Fig. 6 (b)). These beads are, relative to the sliding direction, of the same size range of 2 to 10 µm, as the grooves visible on the Cr60Ni40 flats. EDS revealed that the adhering material (e.g. Area 1, Fig. 6 (b), Tab. 3) contains high amounts of Cr and Ni, while the smooth regions (e.g. Area 2, Fig. 6(b), Tab. 3) are mainly characteristic for the 52100 steel.

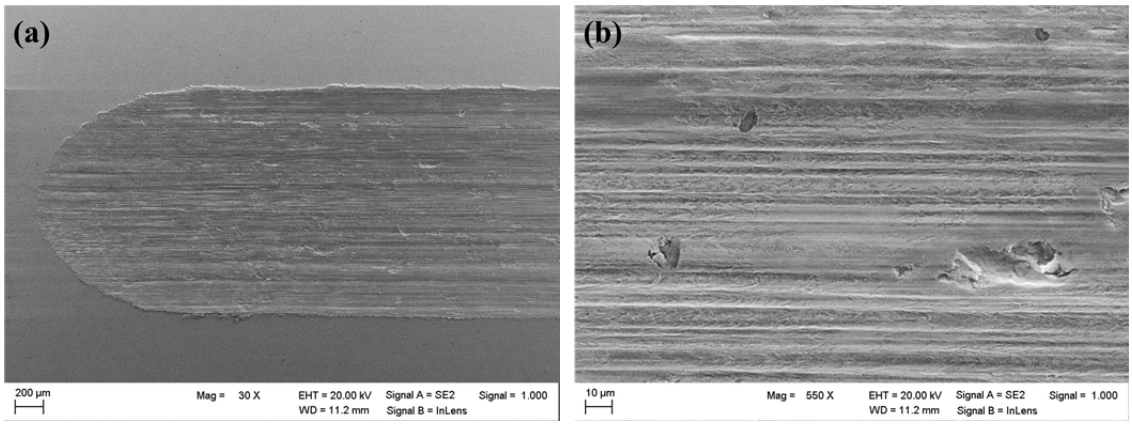

Fig. 5. SEM images of worn surface on cast Cr60Ni40 (60N; 25,000 cycles): grooves and delaminations

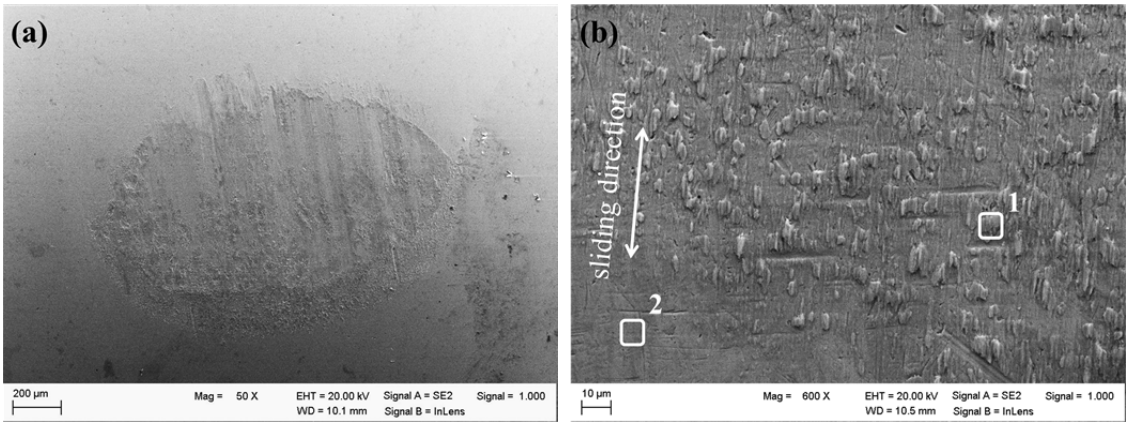

Fig. 6. SEM images of worn surface on the ball corresponding to the flat in Fig. 5: grooves and adhering material

	area 1	area 2
C	5.9	6.6
O	4.6	0.0
Si	4.7	1.6
Cr	27.1	2.3
Mn	0.6	0.3
Fe	33.1	88.3
Ni	24.0	0.9

Tab. 3. EDS measurements as designated in Fig. 6 (b)

Cross sections were prepared parallel to the sliding direction from the worn cast and friction-surfaced samples (Fig. 7, Fig. 8). A deformation gradient parallel to the sliding direction is found underneath the surfaces. Typically, the appearance and the depth of the deformed material vary locally along the wear scar. If clearly visible, the gradient on the cast samples reaches significantly deeper into the material (up to ≈ 50 µm) than on the coatings (up to ≈ 10 µm). In addition bi-convex layers of bright appearance after etching ("white etching layers", WEL) are visible locally underneath the worn surfaces of all samples. They have thicknesses up to 30 µm and, particularly on the cast samples, contain cracks and are partly delaminated (Fig. 7 (b), Fig. 8 (a)). The SEM images in Fig. 9 show parts of WELs on the etched cross sections through wear scars on Cr60Ni40 cast material and an FS coating. EDS measurements were conducted on the indicated areas, and the results are given in Tab. 4. It is obvious that the WELs do not stem from adhesion of the steel counterbody, but consist of elements from the Cr60Ni40 alloy, with increased content of Si, as well as some C and O. From EDS measurements carried out on WELs on six different samples, both cast and FS coatings, the Cr:Ni weight ratio was found to lie consistently at 56:44, with a scatter of ± 1.5 each. The Si content of the WELs ranges between 4.7 and 7.3 wt%, and while up to 1 wt% Si may be present in this alloy, it can be assumed that components from the silicone oil used as lubricant were incorporated into the WELs.

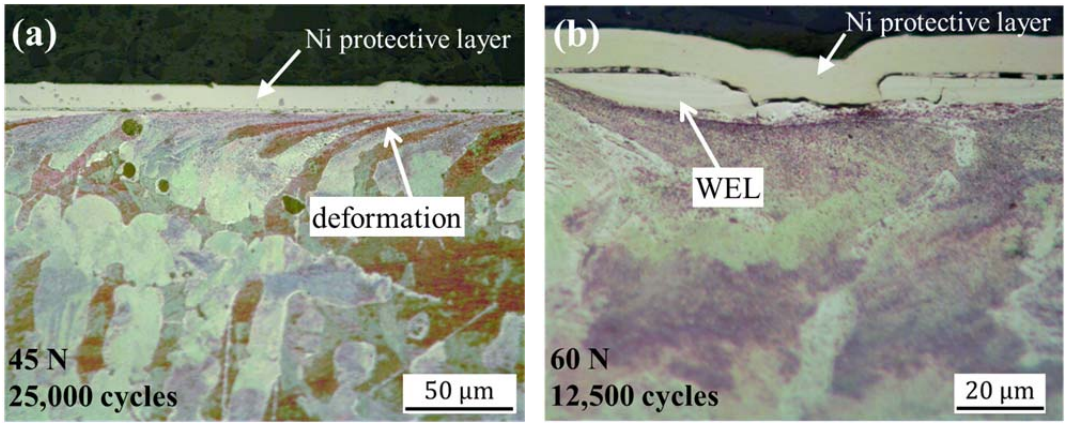

Fig. 7. Cross sections of cast Cr60Ni40 after wear testing, cut parallel to the sliding direction: deformation underneath the worn surface (a) and partly delaminated white etching layer (WEL) (b)

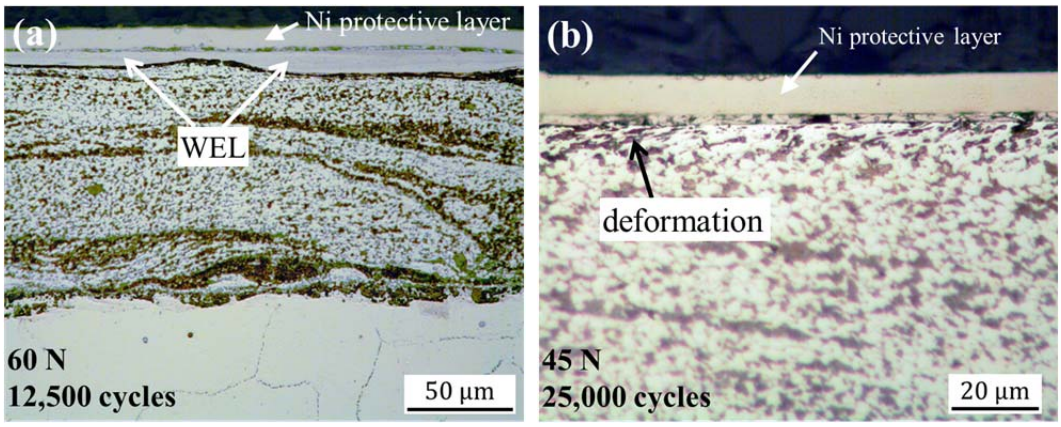

Fig. 8. Cross sections of Cr60Ni40 friction surfacing coating after wear testing, cut parallel to the sliding direction: extensive white etching layers (a) and narrow region of deformed material underneath the worn surface (b)

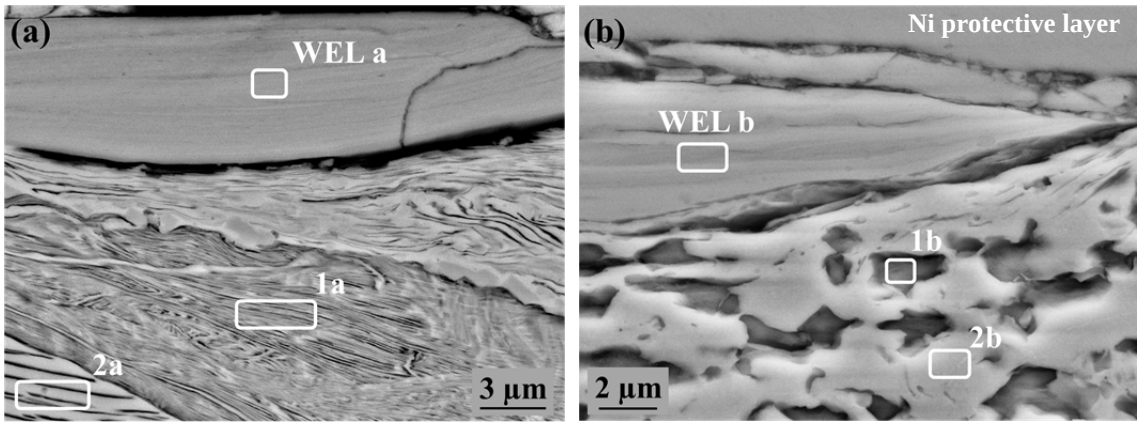

Fig. 9. SEM images of cross sections through worn surfaces from wear tests at 60N for 12,500 cycles, on cast material (a) and an FS coating (b), each showing part of a white etching layer

	WEL a	1a	2a	WEL b	1b	2b
C	6.3	3.0	2.9	4.6	10.3	2.8
O	5.3	2.0	1.5	5.1	4.6	1.8
Si	5.0	0.0	0.3	6.1	1.9	0.5
Cr	47.2	57.7	43.5	46.0	51.1	49.1
Fe	0.4	0.9	1.1	1.4	1.2	1.4
Ni	35.8	36.4	50.7	36.8	30.9	44.4
ratio Cr:Ni	57:43	61:39	46:54	55:45	62:38	53:47

Tab. 4 EDS measurements as designated in Fig. 9

4. Discussion

4.1 Microstructure Evolution during Friction Surfacing

For a more detailed analysis of the microstructure, the reader is referred to [22]. The Cr60Ni40 alloy from centrifugal casting contains regions rich in Cr, which contain small, compact Ni-rich crystals as well as fine, lamellar precipitates and are surrounded by a eutectic. This is characteristic for a typical cast Cr60Ni40 alloy.
During friction surfacing, temperatures close to the melting point are reached, in combination with severe plastic deformation and followed by rapid cooling. This obviously results in the solution and new precipitation of phases. Now the grain size lies in the range of 1 µm, being smaller compared to the cast material. The Cr-rich areas within the coatings still contain fine, lamellar precipitates, but now these are also finer. The bright areas show no signs of eutectic lamellae, which obviously have been dissolved and no corresponding phases have precipitated again. Still, the fcc lattice of Ni governs the crystallographic structure though it is supersaturated by about 52 wt-% Cr. Thus the slightly higher hardness of the coatings can be related to grain size strengthening (by grain refinement) and solid solution strengthening (by supersaturation).

4.2 Wear Behaviour

The wear behaviour of cast material and coatings is comparable. The friction coefficient is effectively the same for all test parameters and both material states, and typical for boundary lubrication. No significant differences of the acting wear mechanisms are found. There is an increase in wear volume both with increasing normal force and test duration. The wear rates first increase with increasing number of cycles and load, but for the high load and test duration decrease again. Both FS coatings and as-cast material follow these trends, while the coatings always exhibit slightly lower wear volumes and rates.

Taking into account the wear scar on cast Cr60Ni40 presented in Fig. 3, it can be estimated that for a wear depth of approximately 70 µm and 25,000 cycles, the average wear rate is about 2.8 nm/cycle. This equals to about 1.4 nm per sliding contact under the given parameters of reciprocating sliding. If the atomic radius of Cr and Ni is taken to

be in the range of 140 pm, it would follow that with each sliding contact in average approximately ten atomic layers have been removed. Thus the wear rate can be assumed to be in the range of mild sliding wear. Grooves, delaminations and material transfer have been found on the contacting surfaces pointing on abrasion, surface fatigue, and adhesion being the acting wear mechanisms [23]. The first and the latter mechanisms are known to generate high wear, and it appears as if the mechanisms do not fit to the measured low wear rates. It must be considered though, that such surface analyses show the acting wear mechanisms but not the timely sequence of their action.

The small beads of material adhering to the balls' surfaces, for which EDS measurements reveal that they originate from the flats, containing high amounts of Cr and Ni, lead to a high surface roughness. If such adhesion takes place during the first few cycles the surfaces of the counterbodies are roughened by transferred Cr60Ni40, which sticks rigidly to the surfaces of the balls. At this stage of the wear process, abrasion probably took place on the balls too, because they are slightly flattened. Such highly deformed asperities can then bring about abrasion, but because of their shallow attacking angle microploughing prevails, leading mainly to plastic deformation and only to some extent to abrasive material removal [23]. Such plastic deformation of the Cr60Ni40 alloy under frictional shear forces is possible, as can be seen in the cross sections (Fig. 7, 8).

Average wear rates for both material states increase with normal force and test duration for three sets of test parameters, and only for the high load and high cycle test they are lower. This implies the occurrence of at least three states of wear; the first involves some abrasive wear of the balls, leading to a flattened contact area. Second, adhesion of Cr60Ni40 leads to roughening of the flat contact area on the balls; wear now mainly occurs on the flats and the wear rate increases. Third, for the highest wear volumes reached at 60 N and 25,000 cycles, a decrease in wear rate is observed, although no change in wear mechanisms is recognizable. This indicates an attenuation of the abrasive, microploughing wear when the trough shaped wear scar on the flats has reached a sufficient depth and width, which can be attributed to a reduction or redistribution of the contact pressure.

Additional wear loss is brought about by WELs generated during microploughing, which then delaminate after being repeatedly loaded due to surface fatigue. Triboxidation can be neglected here, since the silicone oil is chemically inert and does not take up water from the surrounding atmosphere [24]. While the deformation gradient is generally brought about by the cyclic nature of frictional stresses [25] [26], it obviously does not tend towards subsurface cracking. But the WELs can be assumed to be hard and brittle and are, therefore, the origin of the observed delaminations [27]. To clarify the formation mechanisms of the WEL in this load situation, and particularly the cause for the specific chemical composition of these areas, further investigations and high resolution microscopy will be required.

The coatings, although they show the same mechanisms as the cast material, seem to be capable of a more localised shearing. The deformation gradients are thinner and wider WELs with less delaminations are present. This can be explained by the finer and more homogeneous microstructure. The smaller grains may be a better support for the WELs and lead to a more even distribution of shear stresses. The finer distribution of the two different phase regions, which can be expected to have somewhat different mechanical properties, might reduce the subsurface depth of plastic deformation during microploughing. Similar results have been found for wear by cavitation, in which coatings from Cr60Ni40 also showed a better resistance than the cast state [22].

Thus cast and friction-surfaced Cr60Ni40 show a similar wear behaviour under boundary lubricated reciprocating sliding wear, which is characterized mainly by abrasion and surface fatigue and their respective submechanisms microploughing and delaminations.

5. Conclusions

Although very similar mechanisms are observed for the cast and friction-surfaced microstructures of Cr60Ni40, it can be concluded that the microstructural alterations caused by the thermomechanical processing during deposition by friction surfacing contribute to a slightly improved wear resistance of the Cr60Ni40 coatings.

The results of the present study imply that applying coatings (instead of using entire castings) from the high-temperature corrosion and wear resistant Cr60Ni40 onto a ductile substrate is possible and results in an advantageous microstructure within the coatings.

Still, it is not clear whether the finer microstructure remains stable at elevated temperatures. Preliminary heat treatment experiments revealed that lamellar precipitates appear within the supersaturated Ni solid solution. In parallel the fine precipitates, which account for the internal substructure of the Cr-rich phase, coarsen. Thus, further investigations regarding these microstructure alterations at elevated temperatures are necessary. The same is true for analysing the exact sequence of the acting wear mechanisms and contact characteristics by start-stop tests accompanied by contact-mechanical calculations.

Acknowledgements

The authors wish to thank Frank Balter and Hans-Peter Nykamp of University of Duisburg-Essen, Germany, for their efforts in wear testing and metallography. Also we are in debt to Aulis Silvonen, Wärtsilä Finland Oy, Vaasa, Finland, for his cooperation and supply of the cast Cr60Ni40 alloy samples.

References

[1] K.A. Tyayar, Friction welding in the reconditioning of worn components, Svarochnoe Proizvodstov 1/10 (1959) 71-76.

[2] B.M. Jenkins, E.D. Doyle, Hardfacing by low-pressure friction surfacing, Transactions of the Institution of Engineers, Australia. Mechanical Engineering 14/3 (1989) 178-185.

[3] K. Fukakusa, On the characteristics of the rotational contact plane – A fundamental study of friction surfacing, Welding International 10/7 (1996) 524-529.

[4] X.M. Liu, Z.D. Zou, Y.H. Zhang, S.Y. Qu, X.H. Wang, Transferring mechanism of the coating rod in friction surfacing, Surface & Coatings Technology 202 (2008) 1889-1894.

[5] E.D. Nicholas, W.M. Thomas, A review of friction processes for aerospace applications, Int. J. of Materials and Product Technology 13/1-2 (1998) 45-55.

[6] J.Q. Li, T. Shinoda, Underwater friction surfacing, Surface Engineering 16/1 (2000) 31-35.
[7] V.I. Vitanov, N. Javaid, D.J. Stephenson, Application of response surface methodology for the optimisation of micro friction surfacing process, Surface & Coatings Technology 204 (2010) 3501-3508.
[8] P. Lambrineas, P. Jewsbury, Areal coverage using friction surfacing, Journal of Ship Production 8/3 (1992) 131-136.
[9] H. Tokisue, K. Katoh, A. Toshikatsu, T. Usiyama, Mechanical properties of 5052/2017 dissimilar Aluminum alloys deposit by friction surfacing, Materials Transactions 47/3 (2006) 874-882.
[10] D. Nakama, K. Katoh, H. Tokisue, Some Characteristics of AZ31/AZ91 dissimilar Magnesium alloy deposit by friction surfacing, Materials Transactions 49/5 (2008) 1137-1141.
[11] S. Hanke, A. Fischer, M. Beyer, J. dos Santos, Cavitation erosion of NiAl-bronze layers generated by friction surfacing, Wear 273/1 (2011) 32-37.
[12] S. Hanke, M. Beyer, J. dos Santos, A. Fischer, Friction Surfacing of a Cold Work Tool Steel – Microstructure and Sliding Wear Behaviour, Wear 308 (2013) 180–185.
[13] W. Herda, G.L. Swales, Neue Nickel-Chrom-Legierungen mit hoher Beständigkeit gegen Brennstoffaschenkorrosion, Werkstoffe und Korrosion 19/8 (1968) 679-689.
[14] ASTM International, Standard Specification for Castings, Chromium-Nickel Alloy, ASTM 560/A 560 M, 1993.
[15] M.B. Vollaro, D.I. Potter, Phase formation in coevaporated Ni-Cr thin films, Thin Solid Films 239 (1994) 37-46.
[16] P. Nash, The Cr-Ni (Chromium-Nickel) System, Bulletin of Alloy Phase Diagrams 7/5 (1986) 466-476.
[17] L. Kaufman, H. Nesor, Calculation of the Binary Phase Diagrams of Iron, Chromium, Nickel and Cobalt, Zeitschrift für Metallkunde 64/4 (1973) 249-257.
[18] www.calphad.com/nickel-chromium.html, Computational Thermodynamics Inc., Carnegy, USA, 2006.
[19] A.R. Sethuraman, R.J. de Angelis, P.J. Reucroft, Diffraction studies on Ni-Co and Ni-Cr alloy thin films, Journal of Material Research 6/4 (1991) 749-754.
[20] C. Sarbu, S.A. Rau, N. Popescu-Pogrion, M.I. Birjega, The Structure of Flash-Evaporated Cr-Ni (65:35) and Cr-Ni (50:50) Thin Films, Thin Solid Films 28 (1975) 311-322.
[21] M.I. Birjega, M. Alexe, The influence of the argon pressure and substrate temperature on the structure of r.f.-sputtered CrNi(65:35), CrNi(50:50) and CrNi(20:80) thin films, Thin Solid Films 275 (1996) 152-154.
[22] S. Hanke, M. Beyer, A. Silvonen, J.F. dos Santos, A. Fischer, Cavitation erosion of Cr60Ni40 coatings generated by friction surfacing, Wear 301/1-2 (2013) 415-423.
[23] K.H. Zum Gahr, Microstructure and Wear of Materials, Elsevier Science Publishers, Amsterdam, The Netherlands, 1987.
[24] A. J. O'Lenick, Silicones - Basic chemistry and selected applications, Journal of Surfactants and Detergents 3/2 (2000) 229-236.
[25] W.J. Saleski, R.M. Fisher, R.O. Ritchie, G. Thomas, Nature and Origin of Sliding Wear Debris from Steels., in: K.C.Ludema (Ed.) Wear of Materials '83, ASME, 345 East 47th Street, New York, N.Y. 10017, USA, Reston, VA, USA, 1983, pp. 434-445.

[26] A. Fischer, S. Weiss, M.A. Wimmer, The tribological difference between biomedical steels and CoCrMo-alloys, Journal of the Mechanical Behavior of Biomedical Materials 9 (2012) 50-62.
[27] G. Baumann, H.J. Fecht, S. Liebelt, Formation of white etching layers on rail treads, Wear 191 (1996) 133-140.